PROCEEDINGS OF THE YEREVAN STATE UNIVERSITY

Physical and Mathematical Sciences 2016, № 3, p. 84–91

P h y s i c s

ANALYTICAL DESCRIPTION OF PLASMON REFLECTION FROM THE FREE EDGES OF METAL SLIT STRUCTURES

Kh. S. SAHAKYAN *

Chair of the Microwave Radiophysics and Telecommunications YSU, Armenia

In this paper we consider gap surface plasmon (GSP) propagation properties in slit milled in metal. Developed theoretical model allows to derive equations describing the reflection and transmission of the GSP from the free edge of semi-infinite slit or periodic array of semi-infinite slits in metallic host, analytically. Using these equations we calculate the transmitted power efficiency from the slit and from the array of slits. For the conditions when slit width (d) is very small compared to incident wavelength, the transmitted power efficiency is increased proportional with $d^{3/2}$, otherwise the dependence is linear. The relation of transmitted power through periodic array of slits to the transmitted power from single slit depends on slit period for the fixed wavelength. The derived equations give mathematical mechanism to calculate theoretical resonant length, losses and Q-factor of plasmon gap microresonator structures and can be used as a preliminary guideline upon designing plasmon gap microresonator.

***Keywords*:** SPP resonator, sub-wavelength slit, array of slits.

Introduction. Surface Plasmon Polaritons (SPP) allows to confine the field in small sizes far below the wavelength. Gap plasmon microresonators have significantly small mode volume, which highlights the role of subwavelength slit SPP in creating of active nanophotonic devices. These structures prove their usefulness in many applications such as single molecule imaging [1] spectroscopy [2], optical tweezers [3], enhanced surface reactions [4], SPP modulators and detectors [5–7], SPP sources [6]. The high intensity of the light in the dielectric regions makes the system very suitable for creating the base components of plasmonics. The simple structure simplifies the production of the system. All the advantages above with the opportunity to use the metals as an electric contacts make this structure very suitable for optoelectronic applications [7–10].

In the slits the SPP reflects from the free edges of the slit. Multiple reflections can cause Fabri-Perot type of resonance. The Q-factor of such a system is defined by

* E-mail: khachiksah.91@gmail.com

the reflection ratio and loses along the resonator. Resonant length (L_{res}) of the system depends on the wavelength of the SPP in slit (λ_{SPP}) and the phase shift upon the reflection process. The famous $\frac{m\lambda}{2}$ resonant length equation for the standard parallel plate resonator cannot be applied here as the reflection phase shift significantly differs from π [11, 12].

From the aforementioned it is clear that it is necessary to know the amplitude and phase changes upon reflection from the free edge to calculate the Q factor and radiated power from the slit edge. There is significant work done in this field. Analytically was described the reflections from metallic and dielectric gaps [13, 14]. Investigated the SPP reflection from the dielectric-metal-dielectric structure edges using Finite Elements Method (FEM) [15]. Some analytic equations were written in plasmon slit structure that describe SPP reflection and propagation for lossless and dispersion free media [16].

In this letter we present analytically written equations that describe the reflection of the SPP from the free space edge of the slit or periodic array of slits. Equations describe the phase, amplitude changes upon reflection, as well as the ratio of transmitted through the slit (periodic array of slits) intensity to incident intensity.

The SPP Modes of the Slit Structure. Firstly, we examine the reflection of the SPP from the one dimensional single subwavelength slit. A slit of width d is drilled in the $y < 0$ half plane on the metal with ε_m complex permittivity (Fig. 1). The $y > 0$ half plane and the slit are filled with a dielectric medium with ε_d permittivity.

It is assumed, that the already excited SPP directed along with y-axis and having wave vector of $\overrightarrow{k_{in}}$ falls on the free edge of the slit ($y = 0$). Reflected SPP having wave vector of $\overrightarrow{k_r}$ lays in the $y < 0$ half plane.

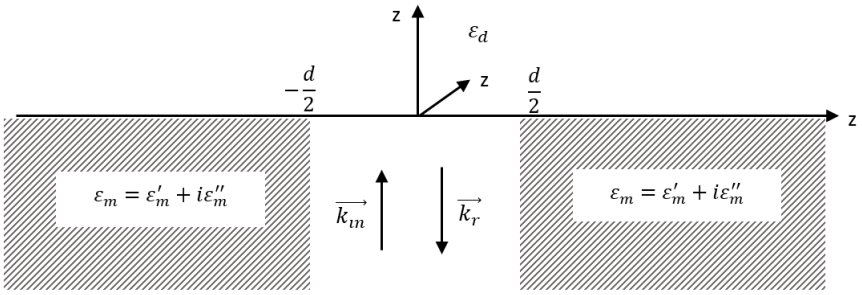

Fig. 1. The structure of the system under study.

In the half plane of $y < 0$ SPP mostly concentrated in the $[-d/2,\ d/2]$ zone, where for the incident SPP we can write:

$$E_x^{in} = B\cosh \varkappa_{in} x e^{i(k_{in}y-\omega t)}, \quad E_y^{in} = \frac{i\varkappa_{in}}{k_{in}} B\sinh \varkappa_{in} x e^{i(k_{in}y-\omega t)}, \tag{1}$$

$$H_z^{in} = -\frac{\sqrt{\varepsilon_d}k_0}{k_{in}} B\cosh \varkappa_{in} x e^{i(k_{in}y-\omega t)}, \tag{2}$$

where $k_0 = \sqrt{\varepsilon_d}\frac{\omega}{c}$, $k_{in}^2 - \varkappa_{in}^2 = \varepsilon_d \frac{\omega^2}{c^2}$ and c is the speed of light at free space.

When $d \ll \lambda$ (i.e. $|\varkappa_{in} d| \ll 1$). The following can be obtained

$$k_{in} \approx k_0 \sqrt{1 + \frac{2}{k_0 d}\sqrt{\frac{\varepsilon_d}{|\varepsilon'_m|}}\, e^{\frac{i\varepsilon''_m}{2|\varepsilon'_m|}}}. \tag{3}$$

Assign:

$$\mu = \frac{2}{k_0 d}\sqrt{\frac{\varepsilon_d}{|\varepsilon'_m|}}. \tag{4}$$

The complex valued wave number k_{in} can be written as $k_{in} = k' + ik''$, where

$$k' = k_0\sqrt{1+\mu}, \quad k'' = k_0 \frac{\mu}{\sqrt{1+\mu}} \cdot \frac{\varepsilon''_m}{2|\varepsilon'_m|}. \tag{5}$$

From the wave equation we have $k_{in}^2 - \varkappa_{in}^2 = \varepsilon_d \dfrac{\omega^2}{c^2}$, where $\varkappa_{in}$ is complex valued as well:

$$\varkappa' = k_0\sqrt{\mu}, \quad \varkappa'' = k_0\sqrt{\mu}\,\frac{\varepsilon''_m}{2|\varepsilon'_m|}, \tag{6}$$

these relations can be easily checked by Maxwell's equations.

Reflection of the SPP from the Edge of Slit. For the reflected wave we have:

$$E_x^r = C\cosh \varkappa_r x e^{-i(k_r y + \omega t)}, \quad E_y^r = -\frac{i\varkappa_r}{k_r} C \sinh \varkappa_r x e^{-i(k_r y+\omega t)}, \tag{7}$$

$$H_z^r = \frac{\sqrt{\varepsilon_d} k_0}{k_r} C \cosh \varkappa_r x e^{-i(k_r y+\omega t)}, \tag{8}$$

$k = k_r = k' + ik'' = k_{in}$ and $\varkappa = \varkappa_r = \varkappa' + i\varkappa'' = \varkappa_{in}$.

The field upper from the slit edge ($y > 0$) can be calculated using quasi-static approximation when $\lambda \gg d$. We assume that in the region of $\rho \ll \lambda$ ($\rho = \sqrt{x^2+y^2}$) the tangential component of electric field is equal to zero at the surface of the metal and has constant value of A at the edge of the slit (Fig. 4):

$$E_x(x,\ y=0) = A\vartheta(d/2 - |x|). \tag{9}$$

It is easy to find a solution for the Poisson equation for the upper half plane, which will satisfy the boundary condition written above

$$E_x^{(+)}(x,\ y) = \frac{Ad}{2\pi} e^{-i\omega t} \int_{-\infty}^{\infty} \frac{\sin(kd/2)}{(kd/2)} e^{ikx - |k|y} dk. \tag{10}$$

After integration for the E_x component we will have:

$$E_x = \frac{A}{\pi}\left\{ \arctan\left[\frac{2\left(\frac{2y}{d}\right)}{\left(\frac{2y}{d}\right)^2 + \left(\frac{2x}{d}\right)^2 - 1}\right] + \pi\vartheta\left(1 - \left(\frac{2y}{d}\right)^2 - \left(\frac{2x}{d}\right)^2\right)\right\} e^{-i\omega t}. \tag{11}$$

The E_y component can be found from the equation $\operatorname{div}\vec{E} = 0$,

$$E_y = -\frac{A}{2\pi}\ln\left[\frac{\left(\frac{2y}{d}\right)^2 + \left(1+\frac{2x}{d}\right)^2}{\left(\frac{2y}{d}\right)^2 + \left(1-\frac{2x}{d}\right)^2}\right] e^{-i\omega t} \quad \text{and} \quad E_z = 0. \tag{12}$$

In the region close to the slit ($y \approx 0$), the fields can be approximated as $E_x = Ae^{-i\omega t}$ and $E_y = -\frac{A}{\pi} \cdot \frac{4x}{d}$.

Using the continuity of the E_x and E_y components of the electric field at the edge of the slit from (1), (7), (11) and (12), we will have:

$$C = \frac{1 - \frac{2+\mu}{\pi\sqrt{1+\mu}} \cdot \frac{\varepsilon_m''}{\sqrt{|\varepsilon_m'|\varepsilon_d}} - \frac{4i}{\pi} \cdot \frac{\sqrt{1+\mu}}{2} \sqrt{\frac{|\varepsilon_m'|}{\varepsilon_d}}}{1 + \frac{2+\mu}{\pi\sqrt{1+\mu}} \cdot \frac{\varepsilon_m''}{\sqrt{|\varepsilon_m'|\varepsilon_d}} + \frac{4i}{\pi} \cdot \frac{\sqrt{1+\mu}}{2} \sqrt{\frac{|\varepsilon_m'|}{\varepsilon_d}}} B, \tag{13}$$

$$A = \frac{2}{1 + \frac{2+\mu}{\pi\sqrt{1+\mu}} \cdot \frac{\varepsilon_m''}{\sqrt{|\varepsilon_m'|\varepsilon_d}} + \frac{4i}{\pi} \cdot \frac{\sqrt{1+\mu}}{2} \sqrt{\frac{|\varepsilon_m'|}{\varepsilon_d}}} B. \tag{14}$$

So, we derived equations that describe the amplitude and the phase of the reflected and transmitted wave. To calculate the ratio of radiated power from the slit to the incident power we write the far field equations ($\rho \gg d$) for the $y > 0$ half plane in spherical coordinate system:

$$E_\varphi = \frac{i\pi d}{\lambda} A H_1^{(2)}(k\rho) e^{-i\omega t},\ H_z = \frac{\pi d}{\lambda} A\sqrt{\varepsilon_d} H_0^{(2)}(k\rho) e^{-i\omega t},\ E_\rho^{(+,-)} = 0, \tag{15}$$

where $H_n^{(2)}$ is Hankel function of the second kind and for $k\rho \gg 1$, can be approximated as:

$$H_n^{(2,1)}(k\rho) \approx \sqrt{\frac{2}{\pi k\rho}} e^{\mp i(k\rho - n\pi/2 - \pi/4)}. \tag{16}$$

The radiation from the slit for the single length is determined by the Pointing vector

$$P_e = \frac{\sqrt{\varepsilon_d} c d^2}{4\lambda} A^2. \tag{17}$$

The incident power to the slit edge is determined from the (1) and (2) and equals to

$$P_0 = \frac{c\sqrt{\varepsilon_d} d}{2\lambda |k_{in}|} B^2. \tag{18}$$

Finally, for the transmitted power we have:

$$T_{21} = \frac{P_e}{P_0} = \frac{\pi^2\sqrt{\varepsilon_d}}{8} \cdot \frac{\varkappa^4 d^2}{k_s}. \tag{19}$$

In the Fig. 2 dependence of the $\frac{P_e}{P_0}$ from the width of the slit (d) is presented. When $\sqrt{\frac{\varepsilon_d}{|\varepsilon_m'|}} \cdot \frac{\lambda}{d} \gg 1$ (which means that in the same conditions $d \ll \lambda$) $P_e/P_0 \sim (d/\lambda)^{3/2}$, otherwise $P_e/P_0 \sim d/\lambda$.

To validate derived equations using finite element method simulation it is expedient to have a finite system. We consider on finite length slit with the length of h. For such a system the plasmon reflects from the upper and lower edges and

can build up Fabry-Perot type of resonator. The resonant length of the resonator is calculated using the equation: $k^{'}h = \varphi$, where φ is the angle of complex valued C/B reflection function in the complex plane. $\varphi = \arctan \dfrac{\Im(C/B)}{\Re(C/B)}$. Loses along the slit length are defined by the term of $e^{-2k^{''}h}$.

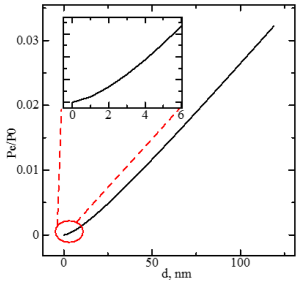

Fig. 2. The dependence of the T_{21} from resonator d width.

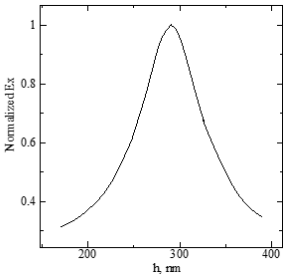

Fig. 3. The dependence of the normalized E_x field from the resonator h length in FEM simulation.

The ratio of the transmitted power through the slit resonator to the incident power can be written in the following form

$$T = \frac{(1-R_{21})^2 e^{-2k^{''}h}}{1-2R_{21}e^{-2k^{''}h}\cos(k^{'}h-\varphi)+{R_{21}}^2 e^{-4k^{''}h}}, \tag{20}$$

where $R_{21} = 1 - T_{21}$. As the $e^{-2k^{''}h} \ll 1$ the (20) can be represented as power series. We keep up to second term of the series and for the resonant length ($k^{'}h = \varphi$) rewrite (20) as

$$T_{\max} = \frac{\left(1-R_{21}\right)^2\left(1-2k^{''}h\right)}{\left(1-R_{21}+2k^{''}hR_{21}\right)^2}. \tag{21}$$

To validate derived expressions we take silver as a metal, which has complex permittivity $\varepsilon_m^{'} = -49.47$, $\varepsilon_m^{''} = 3.6236$ for the wavelength of 1100 nm. As a dielectric medium we take an air ($\varepsilon_d = 1$). So, the $C/B = 0.981507e^{-2.81647i}$, which means that SPP changes the phase by 2.81647 upon reflecting from the edge of the slit. For the resonance length of the system the principal role plays the phase shift upon reflection. Hence, $k^{'}h = 2.81647$ and for resonant length we derive $h = 329$ nm. The absorption of the wave is determined by the equation $e^{-2k^{''}h} = 0.881375$, so, the 0.118625 part of the wave is absorbed during one resonant cycle. To check the result the model with the same parameters is designed using COMSOL Multiphysics as a finite element method software.

The x and y components of the electric field are presented in the Fig. 4. During the simulation we parametrically sweep the length of the slit to get the field intensity dependence curve from the resonator h length. In the Fig. 3 the dependence of the electric field E_x component from the resonator length is shown. It is obvious

that the resonant length is on $h_{res} = 297nm$ (derived equation were foreseen $h_{res} = = 329nm$). We repeated the simulation for the wavelength of 1500 *nm* and recorded $h_{res} = 375$ *nm* for the resonant length (derived equation foreseen $h_{res} = 413$ *nm*). In both cases the deviation from the equations is less than 10%. We also found the main origin of the deviation, which is the approximation done for the electric field component $E_x = Ae^{-i\omega t}$ when $y \approx 0$, to keep equations simple.

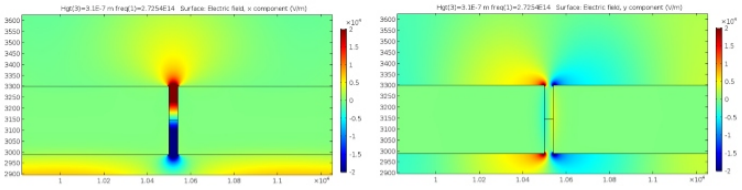

Fig. 4. The E_x (left) and E_y (right) components of the field for the single finite length slit. Width of the slit is 310 *nm*, d = 40 *nm* and the wavelength is equal to 1100 *nm*.

Periodic Array of Slits. Now we analyze periodic array of slits drilled in the metal of half plane $y < 0$. The structure of the system is presented in the Fig. 5. We expend the assumptions we done for single slit structure on the periodic array of slits structure. As for the single slit case SPP propagates through the nth slit in **y** direction and reflects from the $y = 0$ plane. Fields for the incident SPP will be written:

$$E_{xn}^{in} = B\cosh\varkappa_{in}(x-np)e^{i(k_{in}y-\omega t)}, \quad E_y^{in} = \frac{i\varkappa_{in}}{k_{in}}B\sinh\varkappa_{in}(x-np)e^{i(k_{in}y-\omega t)}, \quad (22)$$

$$H_z^{in} = -\frac{\sqrt{\varepsilon_d}k_0}{k_{in}}B\cosh\varkappa_{in}(x-np)e^{i(k_{in}y-\omega t)}. \quad (23)$$

For the reflected wave we have

$$E_{xn}^{r} = C\cosh\varkappa_{in}(x-np)e^{-i(k_{in}y+\omega t)}, \quad E_y^{r} = \frac{i\varkappa_{in}}{k_{in}}C\sinh\varkappa_{in}(x-np)e^{-i(k_{in}y+\omega t)}, \quad (24)$$

$$H_z^{r} = -\frac{\sqrt{\varepsilon_d}k_0}{k_{in}}C\cosh\varkappa_{in}(x-np)e^{-i(k_{in}y+\omega t)}. \quad (25)$$

Like in the single slit case, we assume that in the region of $\rho \ll \lambda$ ($\rho = \sqrt{x^2+y^2}$) the tangential component of electromagnetic field is equal to zero at the surface of the metal and has constant value of A at the edges of the slits (see Fig. 5).

$$E_x = E_0e^{i(k_0y-\omega t)} + \sum_{m=1}^{\infty} b_m e^{-\eta_m}\cos(mqx)e^{-i\omega t}, \quad (26)$$

where $b_m = 2A\dfrac{d}{p}\cdot\dfrac{\sin\left(\frac{\pi d}{p}m\right)}{\frac{\pi d}{p}m}$, $E_0 = \dfrac{d}{p}A$, $q = \dfrac{2\pi}{p}$ and $\eta_m = \sqrt{\left(\frac{2\pi}{p}m\right)^2 - {k_0}^2}$.

For $p \ll \lambda$: $\eta_m = \dfrac{2\pi}{p}m\sqrt{1-\left(\dfrac{p}{m\lambda}\right)^2} \approx \dfrac{2\pi}{p}m$. In the limits of quasi-static approximation and for $y = 0$:

$$E_y \approx -\frac{A}{2\pi}\ln\left[\frac{\sin^2(\pi/p)(d+2x)}{\sin^2(\pi/p)(d-2x)}\right]e^{-i\omega t}. \quad (27)$$

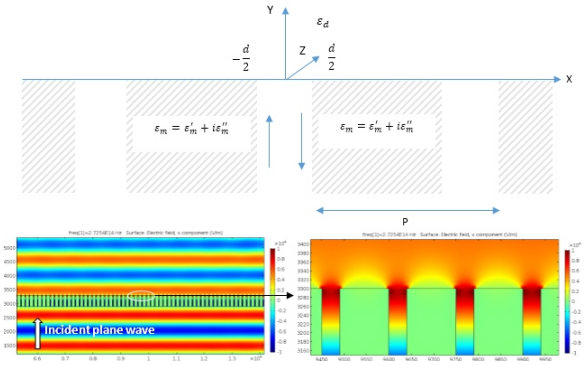

Fig. 5. The structure of the periodic array of slits (top), the overlook of the electric field E_x component (left) and zoomed view of the same (right) for the period of 150 *nm*.

To find C and A terms, we can use the continuity of the fields at the edge of any slit (for ex. $m = 0$). Simplifying the expressions when $y > 0$:

$$E_x = A, \;\; E_y \approx -\frac{4A}{\pi} \cdot \frac{x}{d}. \tag{28}$$

Using continuity condition and keeping terms smaller than $\varkappa^2 d^2$, we will have:

$$C = e^{-2i\varphi} B, \; A = \frac{2B}{\sqrt{1+\tan^2\varphi}} e^{-i\varphi}, \;\; \text{where } \tan\varphi = \frac{4k}{\pi\varkappa^2 d},$$

- for amplitude of the transmitted wave:

$$E_0 = \frac{d}{p} A = \frac{2d/p}{\sqrt{1+\tan^2\varphi}} e^{-i\varphi} B,$$

- for transmitted power from the system of slits:

$$S_{tr} = \frac{4\sqrt{\varepsilon_d}(d/p)^2 B}{1+\tan^2\varphi} \cdot \frac{1}{4\pi c},$$

- for power of the falling wave:

$$S_0 = \frac{k_0}{k} B^2 \frac{d}{p} \cdot \frac{1}{4\pi c},$$

- for ratio of the transmitted power through the periodic slit array system to the incident power:

$$T_{periodic} = \frac{4\sqrt{\varepsilon_d}(d/p)}{1+\tan^2\varphi} \cdot \frac{k}{k_0}, \tag{29}$$

- for ratio of the transmitted power through periodic array of slits to the transmitted power from single slit:

$$\frac{T}{T_{periodic}} = \pi \frac{p}{\lambda}, \tag{30}$$

i.e there is a linear dependence between the ratio and the period of the slits for fixed wavelength.

Conclusion. The derived analytic description of plasmon reflection from the subwavelength slit (periodic array of slits) edge allows obtaining well matching

expressions for the intensity transmission efficiency of the slit, resonant length and losses. Finite element method simulation validates analytical expressions reporting variance not more than 10%. Small variance introduced during the approximations of complex expressions because of our intention to keep model as simple as possible. As a result we have simple to use and yet well enough precise expressions that can serve as a base to design plasmon slit microsystems or periodic plasmon slit array systems at desirable wavelength choosing slit width and height as parameters.

Received 16.06.2016

REFERENCES

1. **Yokota H., Saito K., Yanagida T.** Single Molecule Imaging of Fluorescently Labeled Proteins on Metal by Surface Plasmons in Aqueous Solution. // Phys. Rev. Lett., 1998, v. 80, p. 4606.
2. **Pettinger B., Ren B., Picardi G., Schuster R., Ertl G.** Nanoscale Probing of Adsorbed Species by Tip-Enhanced Raman Spectroscopy. // Phys. Rev. Lett., 2004, v. 92, p. 096101.
3. **Righini M., Volpe G., Girard C., Petrov D., Quidant R.** Surface Plasmon Optical Tweezers: Tunable Optical Manipulation in the Femtonewton Range. // Phys. Rev. Lett., 2008, v. 100, p. 186804.
4. **Cao L., Barsic D.N., Guichard A.R., Brongersma M.L.** Plasmon-Assisted Local Temperature Control to Pattern Individual Semiconductor Nanowires and Carbon Nanotubes. // Nano Lett., 2007, v. 7, p. 3523.
5. **Nikolajsen T., Leosson K., Bozhevolnyi S.I.** Surface Plasmon Polariton Based Modulators and Switches Operating at Telecom Wavelengths. // Appl. Phys. Lett., 2004, v. 85, p. 5833.
6. **Hryciw A., Jun Y.C., Brongersma M.L.** Electrifying Plasmonics on Silicon. // Nat. Mater., 2010, v. 9, p. 3.
7. **Cai W., White J.S., Brongersma M.L.** Compact, High-Speed and Power-Efficient Electrooptic Plasmonic Modulators. // Nano Lett., 2009, v. 9, p. 4403.
8. **Miyazaki H.T., Kurokawa Y.** Controlled Plasmon Resonance in Closed Metal/Insulator/Metal Nanocavities. // Appl. Phys. Lett., 2006, v. 89, p. 211126.
9. **Jun Y.C., Huang K.C.Y., Brongersma M.L.** Plasmonic Beaming and Active Control over Fluorescent Emission. // Nat. Commun., 2011, v. 2, p. 283.
10. **Neutens P., Van Dorpe P., De Vlaminck I., Lagae L., Borghs G.** The Name of the Cited Article. // The Name of Journal, 1987, v. 23, № 8, p. 1366–1376.
11. **Bozhevolnyi S.I., Søndergaard T.** General Properties of Slow-Plasmon Resonant Nanostructures: Nano-Antennas and Resonators. // Opt. Express, 2007, v. 15, p. 10869.
12. **Barnard E.S., White J.S., Chandran A., Brongersma M.L.** Spectral Properties of Plasmonic Resonator Antennas. // Opt. Express, 2008, v. 16, p. 16529.
13. **Jamid H.A., Albader S.J.** Diffraction of Surface Plasmon-Polaritons in an Abruptly Terminated Dielectric-Metal Interface. // IEEE Photon. Tech. Lett., 1995, v. 7, p. 321.
14. **Leskova T., Gapotchenko N.** Fabry-Perot Type Interferrometer for Surface Polaritons: Resonance Effects. // Solid State Commun., 1985, v. 53, p. 351.
15. **Barnard E.S., White J.S., Chandran A., Brongersma M.L.** Spectral Properties of Plasmonic Resonator Antennas. // Opt. Express, 2008, v. 16, p. 16529.
16. **Gordon R.** Light in a Subwavelength Slit in a Metal: Propagation and Reflection. // Phys. Rev. B, 2006, v. 73, p. 153405.